2 Wave storm characterization

2.1 The region of study

The Southern Catalan coast is located on the NW Mediterranean Sea (Figure 2-1).The area is characterized by a complex coastal orography: the main features are the Pyrenees in the north and several abrupt mountain ranges parallel to the coast, which during regional northern winds favour wind channelling down the Ebro River and off the Ebro Delta. The same applies to smaller river valleys, which are associated with 'breaches' in the coastal mountain range. These characteristic northwest land-to-sea winds (*Mistral* in the local vernacular) are particularly intense and persistent, especially during the fall and winter seasons. The highest winds are usually recorded from the east, being usually generated by a cyclone over the western Mediterranean. In the summer, south-westerly winds predominate.

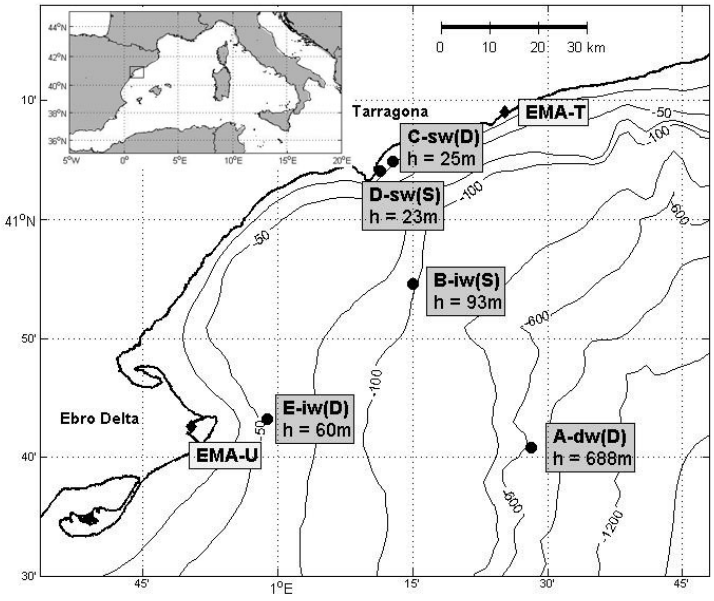

Figure 2-1. Location of the measuring instruments in the study region. B-iw(S), C-sw(D), D-sw(S) and E-iw(D) are wave stations. EMA-T and EMA-U are meteorological stations. A-dw(D) is simultaneously a wave and a meteorological station. The depth at which the buoys were located is denoted by *h*.

The bathymetry presents a narrow continental shelf right in front of Tarragona's harbour: the 700m isobath is only 60km offshore. Towards the south, there is the Ebro Delta, a geographical feature characterized by a gently sloping bathymetry which results in a wider continental shelf. The Delta has been widely studied because of its biological, geological and economical importance. It is one of the largest deltas in the Mediterranean Sea and it is under a lot of external pressure. Jiménez et al. (1997) studied the hydrodynamic processes reshaping it, with special focus on the wave climate.

The directional distribution of waves in the region agrees with the wind patterns and shows a predominance of northwest and eastern wave conditions. The largest waves come from the east and northeast, which are the directions with the largest fetch. Double peaked wave conditions are often observed under strong local northwest winds and onshore east winds (Sánchez-Arcilla et al. 2008). Bimodal events can be defined as the simultaneous existence of two wave systems: two energy peaks at different frequencies and/or directions. In the Ebro Delta region they are indeed very frequent (50% of the time) (Bolaños et al. 2009).

The variations of sea level in the Mediterranean Sea are not as important as in other larger seas (Bolaños et al. 2009). The tidal oscillations are in the order of cm and thus, the area of study was considered as a non-tidal environment. In general, sea level variations, although very important from the engineering point of view, were not taken into account in the present study.

2.2 Available data

2.2.1 Wave measurements

In order to provide a detailed description of wave storms along a perpendicular coastal transect, the campaign RIMA-Med was designed to record wave characteristics along an instrumented transect set perpendicular to Tarragona's coastline. From November 2007 to January 2008 two wave measuring instruments were deployed in the region of study. C-sw(D) was deployed at the entrance of the harbour, and B-iw(S) was deployed 22km offshore. To make it easier for the reader to identify at a glance the characteristics of each station throughout the paper, the capital letter is a reference name for the buoy and it is followed by a pair of lower case letters which indicate the depth of the instrument (*dw*, *iw*, *sw* – deep, intermediate and shallow waters), and a bracketed letter indicating whether the measures taken were directional (*D*) or scalar (*S*).

The transect was completed with two permanent instruments (A-dw(D) and D-sw(S)), which are part of Puertos del Estado (Ports of the State) buoy network. Observations from another operative instrument (E-iw(D)) located south of the first, and over a wider continental shelf, was specifically used to assess spatial variability. This last instrument was especially useful for its directional measurements and the full record provided. It is part of the XIOM network for oceanographic and coastal meteorological measurements (Xarxa d'Instrumentació Oceanogràfica i Meteorològica), which is owned by the Catalan regional government.

Unfortunately, due to operative reasons simultaneous observations from all the instruments could not be obtained. Details on the measuring instruments and its period of measure are provided in Table 2-1; their location is depicted in Figure 2-1.

Table 2-1. Description of the wave measuring instruments. Note that the name of the buoys is a reference to its location and measuring characteristics: the capital letter is a reference name for the buoy; the lower case letters indicate the depth of the instrument (*dw*, *iw*, *sw* – deep, intermediate and shallow waters); and the bracketed letter indicates whether the buoy is directional (*D*) or scalar (*S*).

Instrument	Position	Depth (m)	Period of measure (dd.mm.yy)	Distance from the coast (km)	Characteristics
A-dw(D)	40°41.0N 1°28.1E	688	19.11.07 – 10.01.08	48	Directional wind and wave data
B-iw(S)	40º 54.7N 1º 14.9E	93	4.12.07 – 10.01.08	17	Scalar wave data
C-sw(D)	41°04.9N 1°12.8E	23	30.10.07 – 30.11.08	1	Directional wave data
D-sw(S)	41°04.1N 1°11.3E	24	30.10.07 – 10.01.08	1	Scalar wave data
E-iw(D)	40º43.3N 0º 58. 9E	60	30.10.07 – 10.01.08	10	Directional wave data

2.2.2 Wind Measurements

The wave data set was complemented with measured wind speed (WS) and the direction the wind is coming from (WiD) at three different stations: the deep water meteo-oceanographic buoy A-dw(D), and a couple of coastal automatic meteorological stations: EMA – T (Torredembarra) and EMA – U (Illa de Buda), owned by the Meteorological Service of Catalonia. The location of the stations is shown in Figure 2-1; their main characteristics are provided in Table 2-2.

Table 2-2. Characteristics of the meteorological stations.

Name	Coordinates	Frequency of measure	Location
A-dw(D)	40.68°N 1.47°E	1h	Offshore buoy
EMA-T	41.15°N 1.42°E	30min	Torredembarra
EMA-U	40.71°N 0.84°E	30min	Illa de Buda – Ebro Delta

2.3 Methodology

2.4 Analyzed variables

First, the integrated parameters of the energy spectrum were used to describe wave conditions during the period of measure. The integrated spectral parameters were chosen over the statistical parameters to differentiate opposing wave trains in terms of energetic content. Also, because the wave models used further on resolve the spectral characteristics rather than the surface elevation.

The spectrum of energy is calculated from the sea surface elevation time series, which are represented as discrete Fourier sums. The amount of energy associated to each discrete frequency is calculated using a mathematical analysis called Fast Fourier Transformed (FFT). More information on how to calculate the energy spectrum can be found in Tucker and Pitt (2001).

Wave conditions were studied in terms of the following integrated parameters of the energy spectrum: significant wave height (H_s), peak period (T_p), mean wave direction (MWD) and peak wave direction (PWD). These parameters were obtained from the momentums (m_n) of the energy spectrum using the following expressions:

$$H_s = 4\sqrt{m_0} \qquad T_p = \frac{m_{-2} \cdot m_1}{m_0^2}$$

PWD is the direction the most energetic waves are coming from (peak of the energy spectrum), and MWD is the mean direction (coming from) of all the waves registered. Also, special attention was paid to the evolution of the spectral shape along the instrumented transect. The characterisation of the shape of both the energy and directional spectra was especially useful in situations of crossing sea trains and bimodal spectra. Bimodal situations were identified visually from the energy spectra. The integrated parameters and the energy and directional spectra were obtained using each instrument's own software, when available. Otherwise, WAFO Matlab toolbox was employed (Brodtkorb et al. 2000). WAFO is a Matlab toolbox that calculates the energy and directional spectra and the integrated wave parameters from the raw data time series.

2.4.1 Identifying sea storm events

Hazard situations mainly occur during storm conditions. Therefore, it is important to perfectly understand the physical processes that are occurring during wave storm conditions: how are the storms being generated and how do they propagate and decay. It is also of interest to assess the spatial differences especially in a complex region such as Tarragona's area. During these critical situations the models mis-predictions are more important and its consequences can be more dramatic.

For these reasons, and in order to identify the intervals of time that are later on called 'storm periods', quantitative and qualitative arguments were used on the observations recorded at the instruments. The quantitative method used the criteria locally employed to define a coastal storm

(Gómez et al. 2005; Sánchez-Arcilla et al. 2008; Jiménez et al. 1997). The wave height threshold to be exceeded during more than 6h was taken as 1.5m. The maximum time span in between independent storms during which the threshold was not exceeded was set to 24h. The qualitative method was based on a visual identification with the objective of matching the start of the storm with H_s sharp increase, and the end with H_s decrease. The main reason is the aim to study the storm build up and decay for modelling purposes, for which the initial start time is as important as the peak of the storm. Resulting from these analyses, 5 storm periods were identified, whose details are summarized in Table 2-3.

Table 2-3. Characteristics of the selected storm periods. The directions of wave provenance are NW: Northwest; E: East; S: South;

Storm period	Start and end time	Spectral type	PWD	Maximum H_s at E-iw(D)
1	14 - 18.11.2007	Mainly bimodal	NW + E	2.1m
2	24 - 30.11.2007	Mainly bimodal	NW + E	1.7m
3	07 - 13.12.2007	Mainly unimodal	NW	2.3m
4	15 - 25.12.2007	Unimodal	E	4.1m
5	03 - 06.01.2008	Slightly bimodal	NW + S + E	2.4m

2.5 Results

Table 2-3 summarizes the main characteristics of the five storm periods identified and analyzed below: the maximum H_s at E-iw(D), the measured wave directions and the predominant spectral shapes. The first thing to notice was the high number of bimodal storm periods recorded. Three out of five storm periods presented mixed sea and swell conditions, in agreement with what was reported by Sánchez-Arcilla et al. (2008) and Bolaños et al. (2005). Mixed sea states usually contained a pre-existing eastern swell and superposed northwest, and eventually south, wind-waves.

The first two storms were the typical bimodal events registered in the region: a northwest wind was blowing over a pre-existing but not very important eastern swell (Figure 2-2). Storm 3, however, was characterized by fairly unimodal spectra, originated by a single offshore wind generating wind-waves in a fetch-limited growth conditions scenario. H_s increased with fetch and reached 2.5m high for 20km of fetch at station E-iw(D), and 3.5m high at station A-dw(D), with 55km of fetch (Figure 2-3). These values provide an insight on the importance and magnitude of fetch-limited northwest events in the study region.

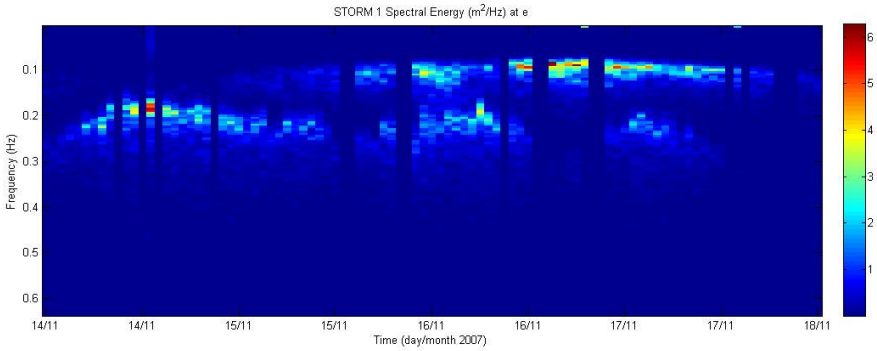

Figure 2-2. Bimodal energy spectra at E-iw(D). The amount of energy (coloured scale) at each frequency (y-axis) is plotted during storm 1. Time is on the x-axis.

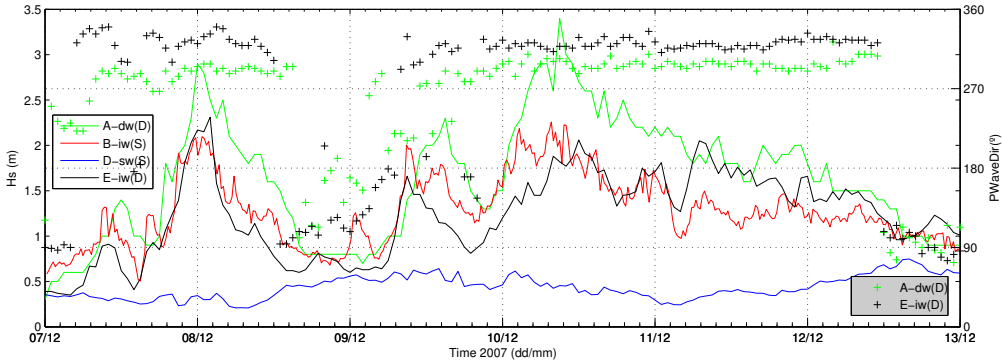

Figure 2-3. H_s (solid lines; left y-axis) and PWD (crosses; right y-axis) during storm 3 at A-dw(D) (green), B-iw(S) (red), D-sw(S) (blue) and E-iw(D) (black).

Storm 4 was clearly unimodal. Wave trains came straight from the east (±30°), and energy spectra were characterized by quite a long high-frequencies tail, because energy was still being input at high frequencies from the wind. This implied that waves were not fully-developed, and some generation was still taking place. In agreement with the longer fetch, H_s was higher than during the other storm periods and it reached 4.1m at station E-iw(D) (Figure 2-4). Unfortunately, during the peak of the storm, observations were not available at the most offshore buoy A-dw(D).

From the analysis of the T_p time series, and as expected, longer T_p (10s) corresponded to eastern swells, and south and northwest events had shorter periods associated (7s and 5s), according to their shorter fetch. This is shown in Figure 2-5, Figure 2-6, and Figure 2-7, where T_p and PWD are plotted together against time.

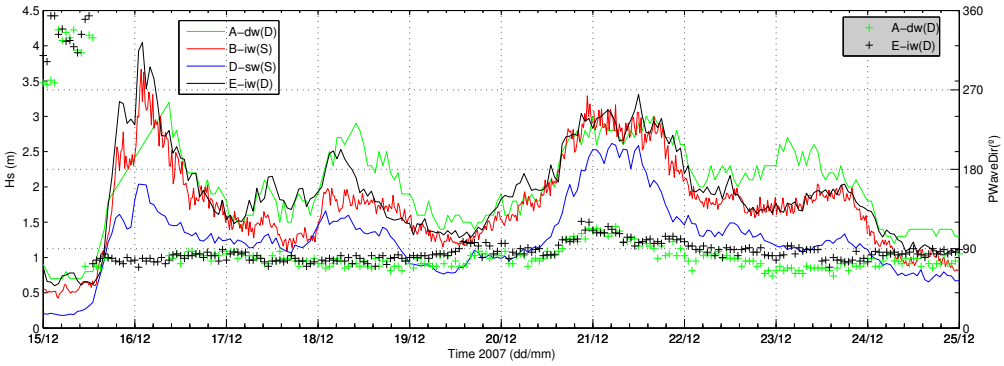

Figure 2-4. H_s (solid lines; left y-axis) and PWD (crosses; right y-axis) during storm 4 at A-dw(D) (green), B-iw(S) (red), D-sw(S) (blue) and E-iw(D) (black).

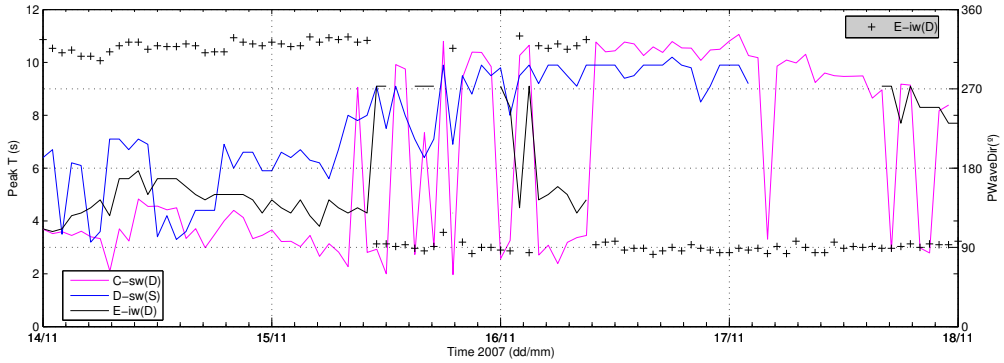

Figure 2-5. T_p (solid lines; left y-axis) and PWD (crosses; right y-axis) during storm 1 at C-sw(D) (magenta), D-sw(S) (blue) and E-iw(D) (black).

The inter-comparison of observations at the different stations along the transect also showed the agreement between the T_p magnitude and the different fetch at each instrument. A clear example is the northwest fetch-limited storm 3 (Figure 2-6), during which T_p at stations B-iw(S) and E-iw(D) was smaller (20km fetch) than at station A-dw(D) (55km fetch). During fully-developed growth events (eastern swells, Figure 2-7 and Figure 2-5), T_p was invariable at all the instruments along the transect, including station C-sw(D) which was sheltered inside the harbour.

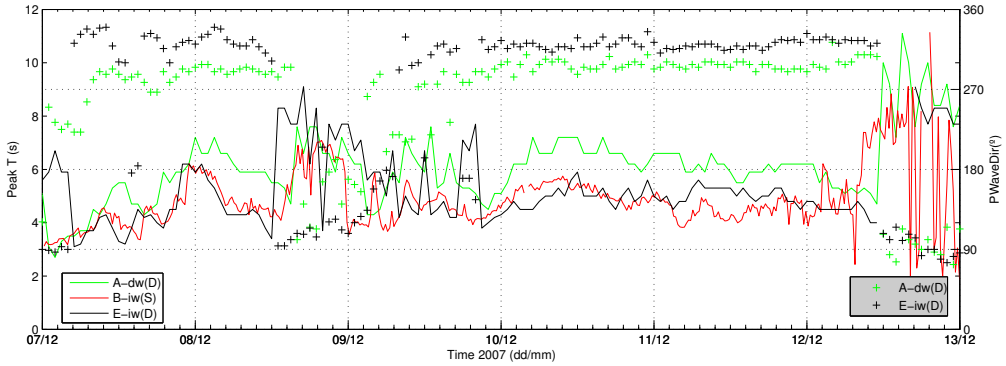

Figure 2-6. T_p (solid lines; left y-axis) and PWD (crosses; right y-axis) at A-dw(D) (green), B-iw(S) (red) and E-iw(D) (black) during storm 3.

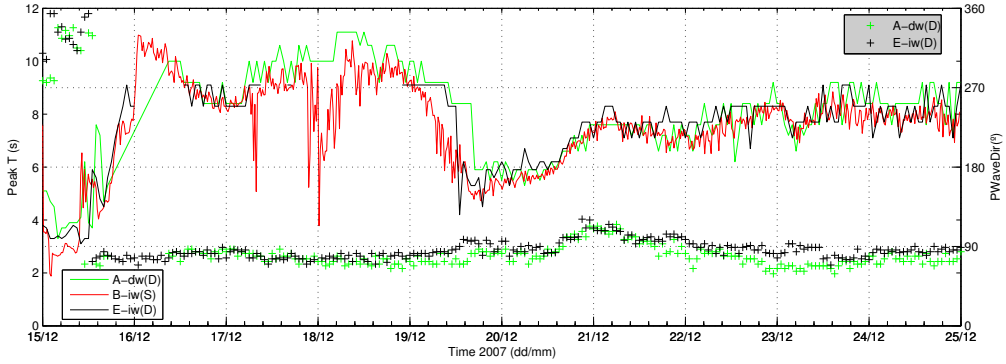

Figure 2-7. T_p (solid lines; left y-axis) and PWD (crosses; right y-axis) at A-dw(D) (green), B-iw(S) (red) and E-iw(D) (black) during storm 4.

An inter-comparison between the time series recorded at all instruments highlighted some further interesting differences. H_s differences at the different instruments could be partially explained in terms of shoaling and fetch, although this was not always possible. Because stations B-iw(S) and E-iw(D) had very similar fetch, observed H_s time series were expected to be similar, but this was not always the case (see Figure 2-3 and Figure 2-4); i.e. the 9th of December a peak of H_s peak was registered at B-iw(S) but not at E-iw(D). Likewise, the 18th of December H_s at E-iw(D) was unexpectedly higher than at B-iw(S).

Besides, a certain PWD deviation was observed between the measurements at stations E-iw(D) and A-dw(D). The largest difference was recorded during storm 3, the unimodal and northwest event during which the PWD at station E-iw(D) was in average 23º more north than PWD at A-dw(D)

(Figure 2-3). During eastern events PWD at E-iw(D) was in average 10º deviated to the south, whereas southern energetic wave trains were 20º deviated towards the east, compared to observations at A-dw(D) (Figure 2-4).

To explain the differences observed between B-iw(S) and E-iw(D), WS and WiD data were analyzed. The two onshore meteorological stations were considered to be representative of the WS along each buoys fetch; i.e. EMA-T was taken as the closest measure of WS along B-iw(S) and A-dw(D) fetch, and EMA-U of E-iw(D). Indeed, the 9th of December 2007 the higher values of H_s recorded at B-iw(S) could be explained by higher WS values at EMA-T (Figure 2-8). However, this was not always true; e.g. the 11th and 18th of December 2007 higher values at E-iw(D) could not be explained using available WS observations. The differences were probably caused by other features of the wind fields that were not captured at the available stations.

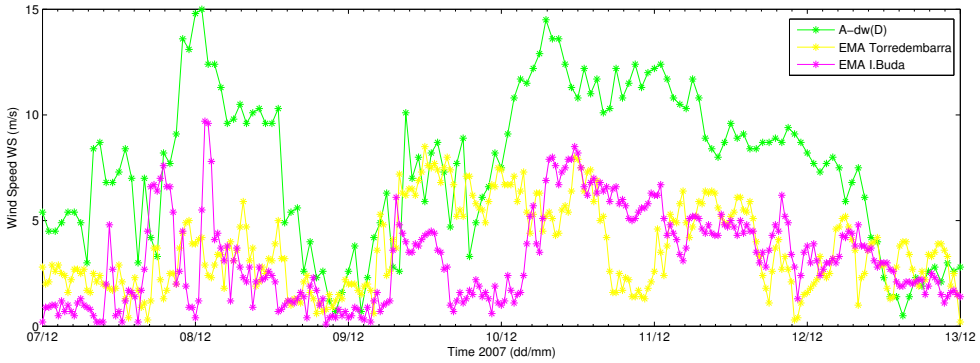

Figure 2-8. WS measurements during storm 3. In green, the observations at offshore buoy A-dw(D), in yellow at EMA-T and in magenta at EMA-U.

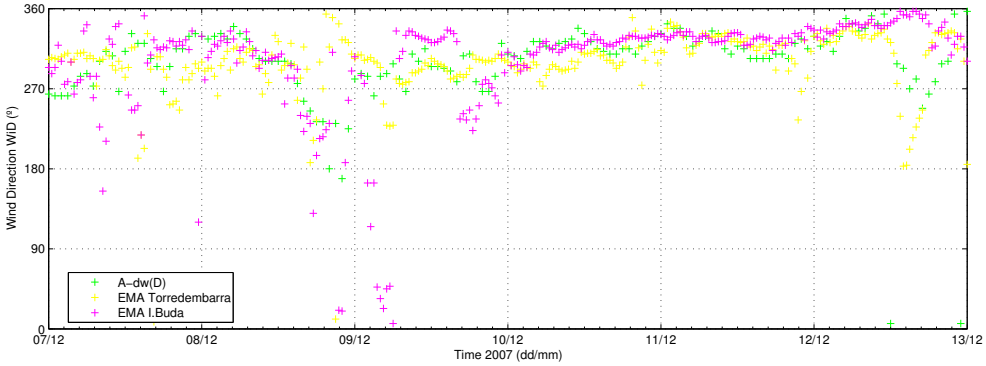

Figure 2-9. WiD observations during storm 4. In green, the observations at offshore buoy A-dw(D), in yellow at EMA-T and in magenta at EMA-U.

Also, PWD deviation could be partially but not fully explained through WiD measurements at the coastal meteorological stations. In Figure 2-9 it can be seen that WiD at EMA-U was blowing slightly more from the north than at EMA-T, although the deviation was not important enough to explain the differences observed in PWD.

The shape of the energy spectra recorded at the different instruments along the transect behaved as expected. During northwest events (fetch-limited growth conditions) the energy increased and the peak frequency decreased for increasing fetch distance (Figure 2-10 (left)). During eastern events (fully-developed growth conditions) the shape of the spectra and the peak frequency were very similar at all the recording instruments (Figure 2-10 (right)). During bimodal events the two characteristics described previously were simultaneously observed for the sea and swell parts of the 'mixed' sea states (Figure 2-11). At station D-iw(S), only 1km offshore, the energy peaks were much lower than at the other locations; the eastern swell components were predominant (peak located around the 0.1Hz frequency range); and trimodal spectra were not uncommon (Figure 2-12).

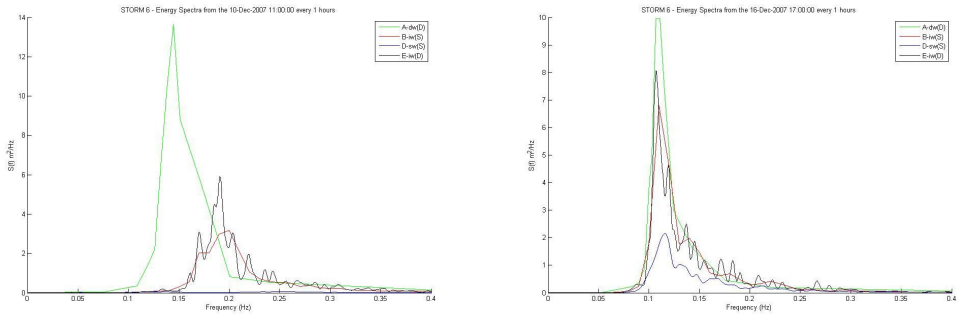

Figure 2-10. Energy spectra at the different instruments during a fetch-limited northwest event (left), and during eastern conditions (right).

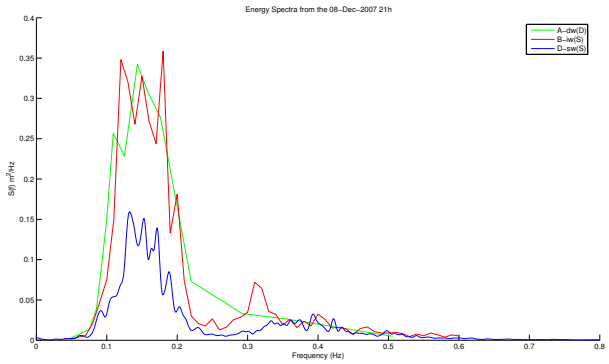

Figure 2-11. Energy spectra at the different instruments during a bimodal event with an eastern swell (low frequency peak) and a less energetic opposing northwest sea (high frequency peak).

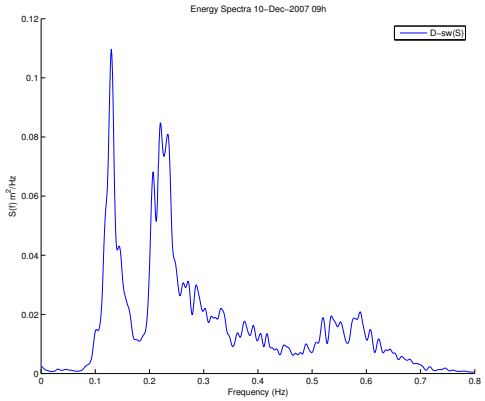

Figure 2-12. Trimodal energy spectrum at D-sw(S) the 10th of December 2007 at 9h.

Unfortunately, directional spectra were only available at E-iw(D). Nonetheless, this information was very valuable in identifying and characterizing bimodal events. Directional spectra at this buoy indicated that bimodal spectra did not only exist during opposing eastern/south swell and northeast sea (Figure 2-13-left and middle panels), but they could also exist when two wave trains from similar but slightly different directions were registered at the same time (Figure 2-13-right panel). Because this possibility was based only in a visual appreciation, it must be further studied and contrasted in the future.

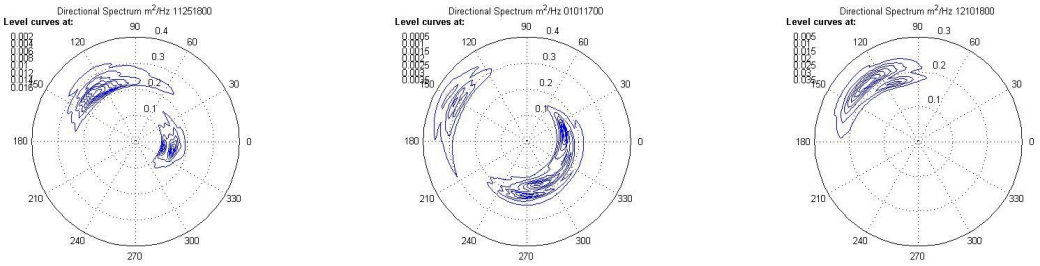

Figure 2-13. Direction Spectra at E-iw(D). The image on the left depicts a typical bimodal spectrum, the central image shows a trimodal spectrum and on the right there is a very-similar-directions two-peaked spectrum.

2.6 Discussion

The main results of this chapter were that wave conditions in the region growed and propagated as expected from the integrated parameters: H_s and T_p increased with fetch and growing sea, whereas T_p was conserved in fully- or almost fully-developed growth conditions. Also, some differences were observed at the different instruments that could not be explained through the available wind observations but would be probably explained by the spatial pattern of the winds. These findings highlighted the high spatial variability of the region.

One of the observed spatial features was a significant deviation of PWD at station A-dw(D) with respect to the measurements at location E-iw(D). This difference could be attributed to wave refraction, spatial wind variability and slanting fetch. The term 'slanting fetch' refers to wind not blowing perfectly perpendicular to the coast. It results in a redistribution of the wave energy across directions to match the direction of the longest fetch (along the coast). On the one hand, the sign of the deviation agreed with the refraction of wave trains approaching E-iw(D), although the deviation observed during storm 3 was larger than expected due to refraction. On the other hand, the largest deviations observed during fetch-limited storm 3 were attributed to different wind directions along the fetch of each buoy, as inferred from the buoy and coastal meteorological stations and the bimodal spectra. Finally, the slanting fetch conditions might also play a significant role as reported by Ardhuin et al. (2007). However, a more detailed study of the wind conditions and how they affect wave train generation and its influence on wave direction is still needed.

The inter-comparison also allowed the identification of differences in H_s at the different locations. Most of the time, these differences could not be explained in terms of WS at the available meteorological stations, and they were usually related to different spectral shapes. Either the energy was much higher or bimodal spectra were recorded at only one of the instruments. These

characteristics confirm the high spatial gradients of the region, and the need for an in-deep study of the processes observed.

The importance of bimodal spectra and its generation and propagation characteristics are of high interest, especially because wave predictions, under these conditions could produce larger errors than during unimodal events (Bolaños and Sánchez-Arcilla 2006). An in-depth understanding of these situations will be addressed in future work.